Distribution of Pentachlorophenol in Phospholipid Bilayers: A Molecular Dynamics Study

Parag Mukhopadhyay, Hans J. Vogel, and D. Peter Tieleman
Department of Biological Sciences, University of Calgary, Calgary, Alberta T2N 1N4, Canada

ABSTRACT Molecular dynamics computer simulations of pentachlorophenol (PCP) in palmitoyl-oleoyl-phosphatidylethanolamine and palmitoyl-oleoyl-phosphatidylcholine lipid bilayers were carried out to investigate the distribution of PCP and the effects of PCP on the phospholipid bilayer structure. Starting from two extreme starting structures, including PCP molecules outside the lipid bilayer, the PCP distribution converges in simulations of up to 50 ns. PCP preferentially occupies the region between the carbonyl groups and the double bonds in the acyl chains of the lipid molecules in the bilayer. In the presence of PCP, the lipid chain order increases somewhat in both chains, and the average tilt angle of the lipid chains decreases. The increase in the lipid chain order in the presence of PCP was more pronounced in the palmitoyl-oleoyl-phosphatidylcholine bilayer compared to the palmitoyl-oleoyl-phosphatidylethanolamine bilayer. The number of *trans* conformations of lipid chain dihedrals does not change significantly. PCP aligns parallel to the alkyl chains of the lipid to optimize the packing in the dense ordered chain region of the bilayer. The hydroxyl group of PCP forms hydrogen bonds with both water and lipid oxygen atoms in the water/lipid interface region.

INTRODUCTION

Interactions between membranes and small moleculles are important in a variety of processes, including drug uptake, passive transport of small molecules, forms of general anesthesia, and accumulation of biopollutants. Microorganisms can be used for biodegradation and bioremediation by breaking down toxic compounds. Much recent research has focused on identifying proteins involved in metabolism of such compounds (Copley, 2000; Denich et al., 2003; Diaz et al., 2001; Wang et al., 2002).

The biophysics of accumulation of toxic compounds in membranes has received less attention but is one of the determinants of metabolism. Partition coefficients of hydrocarbons and other lipophilic compounds in octanol/water, hexadecane/water, and olive oil/water mixtures have been used to predict the effects of these compounds on intact cells. Although these methods, especially octanol/water partition coefficients, show good correlation with biological effects (Osborne et al., 1990; Sikkema et al., 1994), octanol/water partitioning does not provide information on the distribution of a molecule in the inhomogeneous bilayer environment or its effect on lipid properties. Molecular dynamics (MD) computer simulation of lipids is a powerful technique to obtain detailed information about the structure and dynamics of different types of lipid assemblies (Feller, 2000; Saiz et al., 2002; Tieleman et al., 1997). MD simulations have been used to calculate the distribution of water and other small molecules (Jedlovszky and Mezei, 2000; Marrink and Berendsen, 1994, 1996) in the lipid bilayer. Interactions of organic molecules such as dihydropyridines (Aiello et al., 1998), ubiquinone (Soderhall and Laaksonen, 2001), tryptophan (Grossfield and Woolf, 2002), and halothane (Koubi et al., 2000) with lipid bilayers have been studied through molecular dynamics simulations. MD simulations have also been used to investigate the effect of bilayer surface charge density on molecular adsorption, and size and shape selectivity of solute partitioning, diffusion, and permeation across the lipid bilayers (Bassolino-Klimas et al., 1995; Liu et al., 2001; Mitragotri et al., 1999; Xiang and Anderson, 1998; Pratt and Pohorille, 2002; Pohorille et al., 1999).

A major problem with MD simulations aimed at determining the distribution of solutes in the bilayer has been the limited timescale. In this article we calculate, starting from two extreme distributions, the distribution of pentachlorophenol (PCP) in palmitoyl-oleoyl-phosphatidylethanolamine (POPE) and palmitoyl-oleoyl-phosphatidylcholine (POPC) lipid bilayers and obtain converged results on a 30–50 ns timescale. PCP is an environmental pollutant used in wood preservation and is known to induce the alteration of the lipid composition of the cell membrane in some PCP-degrading *Sphingomonas* species isolates UG25 and UG30 (Lohmeier-Vogel et al., 2001). It has also been reported that PCP can alter the cytoplasmic membrane fluidity in certain bacterial strains (Trevors, 1983). Here we investigate the distribution of PCP in the bilayer and the effects of PCP on the phospholipid bilayer structure, and interpret the results in terms of the molecular interactions between PCP and the lipid molecules. Such detailed MD simulations will help in understanding the physical basis for cytoplasmic membrane modifications, one of the adaptive mechanisms of bacteria in the presence of xenobiotic compounds (Hazel and Williams, 1990; Mishra and Kaur, 1991; Sajbidor, 1997).

Submitted June 26, 2003, and accepted for publication September 26, 2003.

Address reprint requests to D. Peter Tieleman, Fax: 403-289-9311; E-mail: tieleman@ucalgary.ca.

0006-3495/04/01/337/09 $2.00

MATERIALS AND METHODS

Simulation setup

Six simulations were carried out: 1), a POPE bilayer consisting of 128 lipids and 6032 water molecules; 2), and 3), two different starting configurations of

15 PCP molecules in a POPE bilayer (Fig. 1), POPE-A and POPE-B; 4), a POPC bilayer consisting of 128 lipids and 2460 water molecules; 5), and 6), two different starting configurations of 15 PCP molecules in a POPC bilayer, with starting configurations similar to the PCP-POPE systems, POPC-A and POPC-B, respectively. All of the PCP molecules were inserted manually inside and outside the lipid bilayer. All of the starting structures were energy minimized, before the MD simulations, to avoid unfavorable contacts between molecules.

Simulation procedure

All simulations were carried out using the GROMACS 3.0 software package (Berendsen et al., 1995; Lindahl et al., 2001). In all simulations a leapfrog (Hockney et al., 1974) integrator was used with a 2-fs time step. All bonds were constrained to their equilibrium values using the SETTLE algorithm (Miyamoto and Kollman, 1992) for water and the LINCS algorithm for all other bonds (Hess et al., 1997). A twin-range cutoff was used for the Lennard-Jones interactions, with interactions within 0.9 nm evaluated every step and interactions between 0.9 and 1.4 nm evaluated every 10 steps. The electrostatic interactions were evaluated using the particle mesh Ewald method (Darden et al., 1993; Essmann et al., 1995). The real-space interactions were evaluated using a 0.9-nm cutoff, and the reciprocal-space interactions were evaluated on a 0.12-nm grid with fourth-order spline interpolation. The simulations were performed with anisotropic pressure coupling, to 1 bar independently in x, y, and z directions, which allowed the area per lipid to fluctuate during the simulation. Each component of the system (i.e., PCP, lipids, and water) was coupled separately to a temperature bath at 298 K, using the Berendsen thermostat (Berendsen et al., 1984), with a coupling constant of 0.1 ps. The SPC (Berendsen et al., 1981) water model was used in all of the simulations. The lipid forcefield parameters were taken from Berger et al. (Berger et al., 1997). The partial charges on PCP (Table 1) were calculated using the Gaussian program (Frisch et al., 1998) at the Hartree-Fock level with the 6-31G* basis set and charge partitioning using the MK method (Besler et al., 1990). As shown in Table 1, the magnitude of the charges on the atoms in PCP molecules is small. The electron withdrawing tendencies of the chlorine atoms in PCP also reduce the potential for the formation of cation-π–type interactions with these molecules

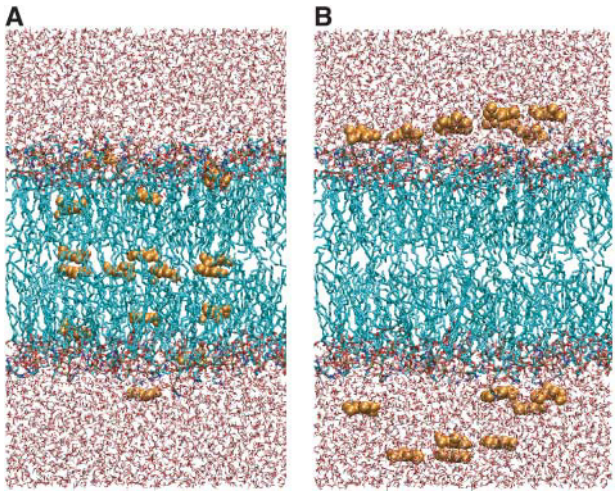

FIGURE 1 The two starting configurations of the PCP-POPE bilayer system. (*A*) PCP placed inside the hydrocarbon core and the interface region of the bilayer (system POPE-A). (*B*) PCP placed in the bulk water region (system POPE-B). PCP is shown as orange van der Waals spheres. Water is represented as red and white lines. The lipid bilayer is drawn as cyan lines for hydrocarbon chains, red and blue lines for the interface region.

TABLE 1 Charge distribution in pentachlorophenol

Atom number*	Partial charges calculated at 6-31G* level with MK fitting	Partial charges used in the simulation
Cl	−0.2542	−0.25
Cl2	−0.02718	−0.03
C3	0.78774	0.80
O4	−0.78953	−0.80
H5	0.52417	0.68
C6	−0.30135	−0.30
Cl7	−0.06136	−0.10
C8	0.18969	0.20
Cl9	−0.05323	−0.10
C10	−0.07771	−0.10
Cl11	−0.06180	−0.10
C12	0.18967	0.20
C13	−0.06483	−0.10

*Atom number corresponds to the atom numbering on PCP as shown in Fig. 2.

(Mecozzi et al., 1996). The Lennard-Jones parameters for PCP were taken from the OPLS all-atom forcefield (Jorgensen et al., 1996), and the bonded parameters were taken from the GROMOS87 forcefield (van Gunsteren et al., 1996). Two 15-ns simulations of the pure POPE and POPC bilayers were carried out, followed by two simulations of 30 ns and 50 ns each for the PCP-POPE systems, and two simulations of 40 ns each for the PCP-POPC systems, from the starting configurations of Fig. 1, *A* and *B*. The starting structures for the pure POPC lipid bilayer were taken from previously equilibrated systems and can be downloaded from http://moose.bio.ucalgary.ca/Downloads/ (file popc128b.pdb). The POPE bilayer started from a previous, unpublished simulation; the final structure is available from http://moose.bio.ucalgary.ca. The 15-ns simulations of the pure POPE and POPC bilayers were carried out with the same set of parameters and under the same simulation conditions as for the PCP-bilayer systems, so that a direct comparison could be made between the bilayers with and without PCP. Coordinates were saved every picosecond. Analyses of the trajectories generated from the MD simulations were done with GROMACS programs. Molecular graphics were made with the VMD program (Humphrey et al., 1996).

RESULTS

Characterization of the membrane systems

For the PCP-POPC systems, the two different starting configurations converged to give a similar area per lipid of 0.62 ± 0.01 nm^2 after 20ns of simulation. The last 20 ns of the POPC-A and POPC-B trajectories were thus used for analysis of the PCP-POPC system. For the PCP-POPE systems, the two different starting configurations converged to give an area per lipid of 0.49 ± 0.01 nm^2 over the last 15 ns and 25 ns of the POPE-A and POPE-B simulations, respectively. The last 15 ns and 25 ns of the POPE-A and POPE-B trajectories were thus used for analysis of the PCP-POPE system. Smejtek et al. found that the area per lipid for the egg-phosphatidylcholine bilayer does not change significantly in the presence of PCP (Smejtek and Wang, 1993). An experimental estimate of the area per lipid for fully hydrated POPC is 0.64 ± 0.01nm^2 (Konig et al., 1997). The average areas per lipid for POPC from the

simulations of the PCP-POPC systems were the same as that obtained from the pure POPC bilayer simulation. The average areas per lipid for POPE from the simulation of the PCP-POPE systems were also the same as that obtained from the pure POPE lipid bilayer simulation. An experimental estimate of the area per lipid for POPE bilayer in the lamellar phase at 30°C is 0.56 nm^2 (Rand and Parsegian, 1989). The area per lipid obtained from the pure POPE lipid bilayer simulation at 25°C is 10%–14% less than the experimental value. This experimental value is likely to have a significant error margin, based on the range of values obtained for lipids such as dipalmitoylphosphatidylcholine for which relatively accurate values from diffraction are available (Nagle and Tristram-Nagle, 2000). The simulation value would increase somewhat at a higher temperature of 30°C and also depends on details of the simulation method (Anézo et al., 2003) that can only be calibrated based on accurate experimental data. Given the similar distribution of PCP in POPE and POPC lipid bilayer (see the following section, Position of PCP in the Lipid Bilayers), we do not think that simulations of POPE bilayer performed at a fixed area per lipid of 0.56 nm^2 would give significantly different results.

Position of PCP in the lipid bilayers

The structure and definition of the groups used for analysis of the PCP-POPC and PCP-POPE system's density profiles are shown in Fig. 2. Fig. 3 shows the average density profiles along the direction normal to the bilayer surface, *Z*, for the various lipid groups and the PCP molecules. For the POPC-B system, 14 out of the 15 PCP molecules were inserted into the bilayer after 20 ns of simulation. The density profiles of the POPC-A and POPC-B systems (Fig. 3, *A* and *B*), averaged over the last 20 ns of the simulations, are nearly identical, indicating convergence of the distribution of PCP in the POPC bilayer. The distribution of PCP in the POPC bilayer is symmetrical with respect to the two leaflets of the bilayer. For the POPE-B system, 12 out of the 15 PCP molecules were inserted into the bilayer after 25 ns of simulation. The density

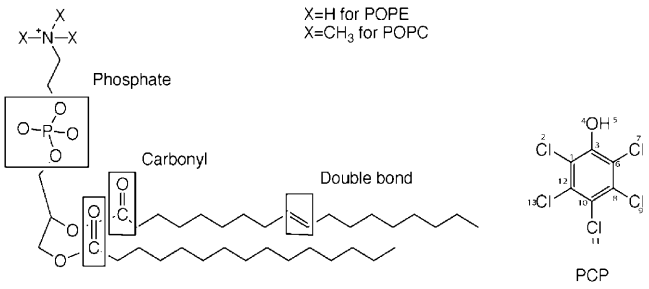

FIGURE 2 The chemical structure of POPC, POPE, and PCP. Note that the double bond is *cis*. The names and structure of the groups used in the analysis of the density profiles in Fig. 3 are shown. The numbering of the atoms in PCP corresponds to the charge distribution of Table1.

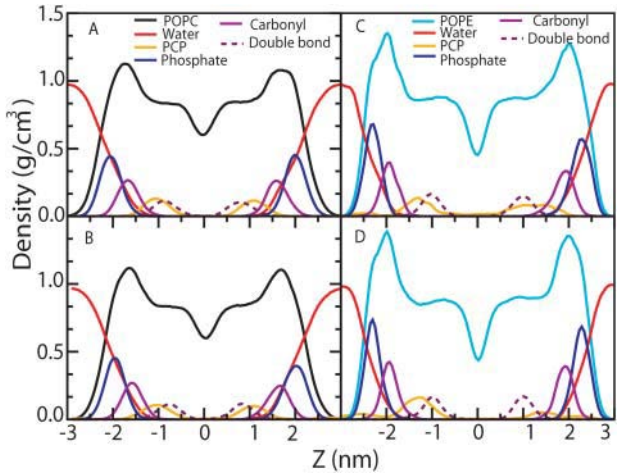

FIGURE 3 Density profiles of the various groups (as defined in Fig. 2), along the bilayer normal for POPC (*A* and *B*) and POPE (*C* and *D*), starting from the two different configurations of Fig. 1. For the POPC bilayer, the density profiles were averaged over the last 20 ns of the trajectories, from the two different starting configurations of Fig. 1. For the POPE bilayer, the density profiles were averaged over the last 15 ns and 20 ns of the trajectories, from the two different initial configurations of Fig. 1 *A* and Fig. 1 *B*, respectively.

profiles of the POPE-A and POPE-B systems (Fig. 3, *C* and *D*), averaged over the last 15 ns and 25 ns of simulations are similar, indicating convergence of the distribution of PCP inside the POPE bilayer, although equilibration between PCP in water and in the bilayer is slower. The distribution of PCP in the POPE-A system was more symmetrical with respect to the two leaflets of the bilayer than in the POPE-B system. As shown in Fig. 3, the distribution of PCP in the POPC and POPE bilayers is quite similar.

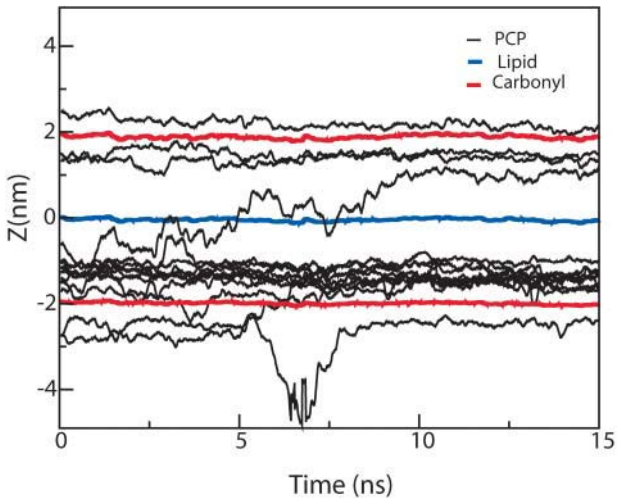

FIGURE 4 The center of mass position of individual PCP molecules over the last 15 ns of the PCP-POPE bilayer system from the starting configuration of Fig. 1 *B*, projected onto the bilayer normal direction, *Z*. The center of mass position of the POPE lipid bilayer and the carbonyl groups of the acyl chains are also shown.

Fig. 4 shows the trajectory of the center of mass along the membrane normal of the PCP molecules in the POPE-B system for the last 15 ns of the simulation. Twelve out of the fifteen PCP molecules that move into the lipid bilayer occupy positions below the carbonyl group of the acyl chains, two of the PCP molecules occupy positions in the interface region, and one PCP molecule is still in the water region by the end of the simulation. Fig. 4 also shows one of the PCP molecules migrating from one leaflet to the other leaflet of the bilayer. Similar dynamics are observed in the POPC-B. In both the POPC-A and POPE-A systems, seven PCP molecules, which were placed in the center of the bilayer, move away from the center of the bilayer to the region below the carbonyl groups within the first 5 ns, and stay inside the hydrocarbon core of the lipid bilayers for the remainder of the simulation. Thus PCP does not show any preference to stay in the center of the lipid bilayer, which has the largest amount of free volume (Marrink et al., 1996). Fig. 3, *A–D* shows that the distribution of PCP has significant overlap with the distribution of the carbonyl groups and the double bonds of the alkyl chain of the POPC and POPE bilayers. Thus PCP occupies the region between the carbonyl groups and the double bond in the alkyl chains of the lipid molecules. Because in both sets of simulations PCP ends up inside the hydrocarbon core of the bilayer, the POPE-A and POPC-A trajectories were used for the remainder of the analyses below.

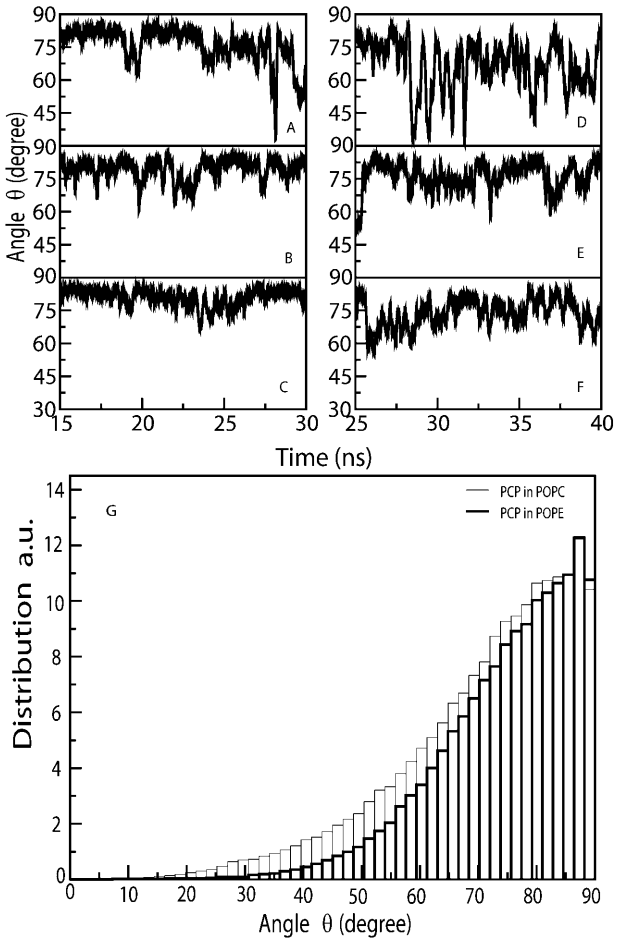

FIGURE 5 Orientation of PCP in the POPE (*A–C*) and POPC (*D–F*) bilayers, determined by the angle θ between the vector normal to the aromatic ring and the bilayer normal, averaged over the last 15 ns of the POPE-A and POPC-A trajectories. *G* shows the distribution of the angle θ of all the PCP molecules that are inside the lipid bilayers for the POPC-A and POPE-A systems.

Interactions of PCP with the local environment in the bilayer

The orientation of PCP molecules relative to the bilayer normal can be described by the angle θ between the vector normal to the PCP ring and the bilayer normal. Fig. 5 shows θ for three PCP molecules in the POPE (Fig. 5, *A–C*) and POPC (Fig. 5, *D–F*) bilayers for the last 15 ns of the trajectories.

In the POPE and POPC bilayers, the vector normal to the PCP aromatic ring makes an average angle of 80° and 70°, respectively, with the bilayer normal. The average tilt angles of the palmitoyl alkyl chains (see the following section, Effect of PCP on the Lipid Bilayer Structure) in the POPE and POPC bilayers in the presence of PCP are 19° and 32°, respectively. As the vector normal to the plane of the aromatic ring makes an average angle of 80° with the bilayer normal in the PCP-POPE system, a vector parallel to the plane of the aromatic ring should make an average angle of 10° with the bilayer normal, because the two vectors are orthogonal to each other. Thus the plane of the aromatic ring of PCP aligns almost parallel to the alkyl chains in the POPE bilayer. Similar alignment is found in the POPC systems. Fig. 5 *G* shows the distribution of the angle θ for all the PCP

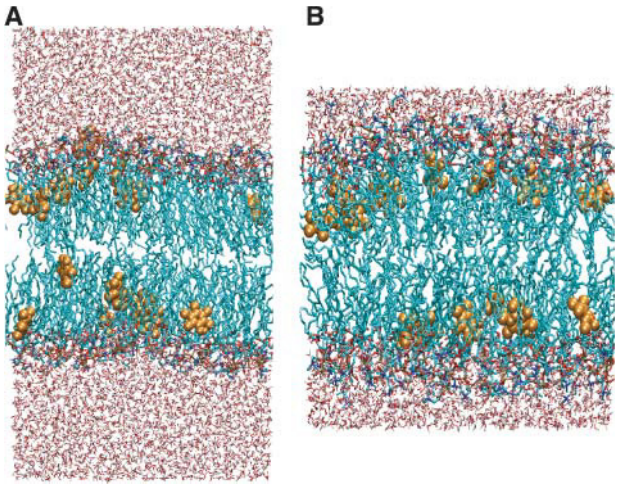

FIGURE 6 Snapshots of the distribution of PCP in the POPE-A system (*A*) taken at 30 ns, and in the POPC-A system (*B*) taken at 40 ns. PCP is drawn as van der Waals spheres. Lipids are drawn as cyan lines for hydrocarbon chains, red and blue lines for the interface region.

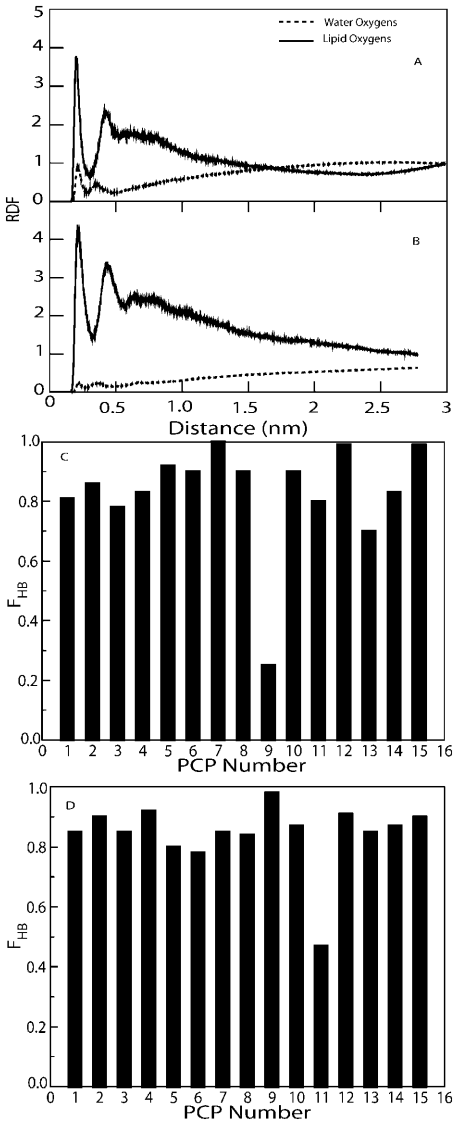

FIGURE 7 Radial distribution functions for water and lipid oxygen atoms around the hydrogen atom of the hydroxyl group of PCP in POPC (*A*) and POPE (*B*) bilayers, averaged over the last 20 ns and 15 ns of the POPC-A and POPE-A trajectories, respectively. (*C* and *D*) Fraction (F_{HB}) of time PCP hydroxyl group forms hydrogen bond with lipid and water oxygen atoms in the POPC-A system (*C*), averaged over the last 20 ns, and in the POPE-A system (*D*), averaged over the last 15 ns.

molecules that are inside the lipid bilayer. The slightly broader distribution of the angle θ in POPC bilayer compared to POPE bilayer shows that PCP has greater orientational freedom in the POPC bilayer. Fig. 6 shows snapshots of the distribution of PCP in POPE (Fig. 6 *A*) and POPC (Fig. 6 *B*) bilayers. The parallel alignment of the aromatic rings with the lipid chains is clearly shown. This kind of alignment of the ring with the lipid chains is most likely to attain optimal packing of PCP in the dense region of the membrane.

To investigate the interactions of the polar hydroxyl group (OH) of PCP in the nonpolar environment of the alkyl chains, we calculated radial distribution functions of the potential hydrogen bonding partners around PCP. Fig. 7 shows the radial distribution function (RDF) for the oxygen atoms of the lipid and water molecules around the hydrogen atom of the hydroxyl group of PCP in the POPC (Fig. 7 *A*) and the POPE (Fig. 7 *B*) bilayers. The first peak in the RDFs occurs around 0.24 nm, within hydrogen bonding distance. The difference in the RDFs of the water oxygen atoms around the hydroxyl group of PCP in the POPC and POPE bilayers is due to the difference in the packing of the lipids in the two bilayers: the larger surface area per lipid for the POPC bilayer compared to the POPE bilayer results in a greater number of water molecules being present at the interface region of the POPC bilayer. To further analyze the hydrogen bonding, we calculated the fraction of the time (F_{HB}) the hydroxyl group of PCP remains hydrogen bonded with either lipid or water oxygen (Fig. 7, *C* and *D*) atoms in the POPC and POPE bilayers. A cutoff distance of 0.32 nm between the donor and acceptor atoms, corresponding to the first minima in the RDF (Fig. 7, *A* and *B*), and the cutoff angle of 60° between the H, donor and acceptor atoms were used as the geometrical hydrogen bond criterion for calculating the number of hydrogen bonds. The fraction $F_{HB} = n_H/n_T$ (Randa et al., 1999), where n_H equals the total number of time steps during which the hydroxyl group of a PCP molecule was observed to form hydrogen bonds, either with lipid or water oxygen, and n_T equals the total number of time steps in the simulation is shown in Fig. 7, *C* and *D*. The hydroxyl group of PCP spends more than 80% of the simulation time (*solid bars*) hydrogen bonded to the oxygen atoms in the POPC and POPE bilayers, of which 60–70% were with the lipid oxygen and the rest, 20–10%,

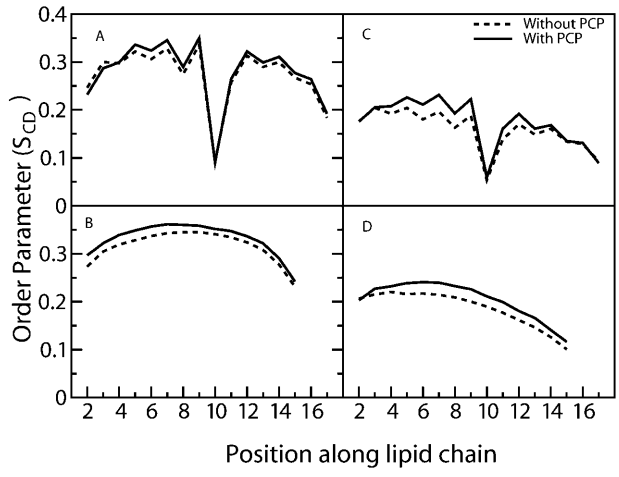

FIGURE 8 Comparison of the deuterium order parameter (S_{CD}) of the alkyl chains in the POPE (*A*, oleoyl; *B*, palmitoyl) and POPC (*C*, oleoyl; *D*, palmitoyl) with and without PCP. S_{CD} of the alkyl chains in the lipid bilayers in the presence of PCP was obtained over the last 20 ns and 15 ns of the POPC-A and POPE-A trajectories, respectively. S_{CD} of the alkyl chains in the pure POPE and POPC bilayers was obtained over the last 10 ns of the pure bilayer simulations.

were with the water oxygen atoms found in the water/lipid interface.

Effect of PCP on the lipid bilayer structure

For the POPC bilayer, the difference in the distance between the center of mass of the polar groups in the two leaflets of the bilayer, in the presence and absence of PCP, is ~0.03 nm for the phosphodiester group; 0.04 nm for the choline headgroups, $N(CH_3)$; with no significant difference for the carbonyl groups, C=O. For the POPE bilayer, these differences were ~0.03 nm for the phosphodiester group, PO_4; 0.06 nm for the ethanolamine headgroups, NH_3; and 0.04 nm for the carbonyl groups, C=O. Thus there is a very small increase in the bilayer thickness in the presence of PCP. The water structure around the headgroups of the POPC and POPE lipids in the bilayers, calculated from the RDF of the water oxygen atoms around the choline, ethanolamine, phosphodiester, and carbonyl groups of the lipid molecules, does not significantly change in the presence of PCP molecules in the bilayers (data not shown).

The effect of PCP on the lipid packing in the bilayer can be deduced from changes in the deuterium order parameter, S_{CD}, along the lipid chain (Boden et al., 1991). The S_{CD} order parameters were calculated using the equation:

$$S_{CD} = \langle 3/2(\cos^2\theta) - 1/2 \rangle, \quad (1)$$

where θ is the angle between the CD bond and the bilayer normal. Deuterium positions were constructed from the neighboring carbons assuming ideal geometries. The brackets imply averaging over time and molecules. Fig. 8 shows the averaged S_{CD} parameters of the alkyl chains in the POPE-A (Fig. 8, *A–B*) and POPC-A (Fig. 8, *C–D*) systems and compares them to the S_{CD} parameters of the alkyl chains in the pure bilayers.

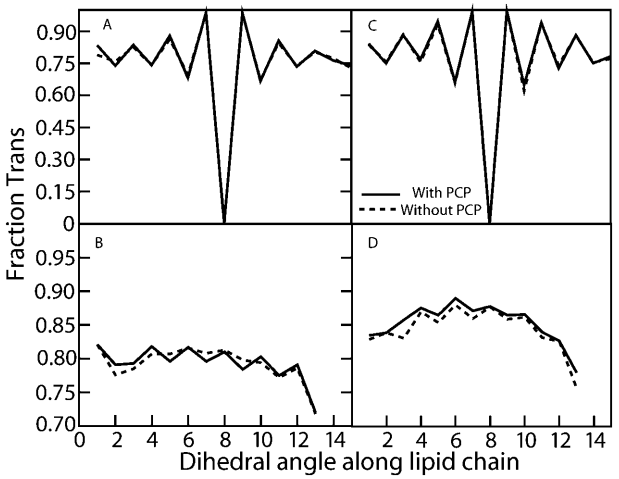

FIGURE 9 Comparison of the fraction of dihedral angles in *trans* conformation along the alkyl chains in the POPC (*A*, oleoyl; *B*, palmitoyl) and POPE (*C*, oleoyl; *D*, palmitoyl) bilayers with and without PCP. The fraction of *trans* dihedral in the presence of PCP was obtained over the last 20 ns and 15 ns of the POPC-A and POPE-A trajectories. The fraction of *trans* dihedrals in the pure POPE and POPC bilayers were obtained over the last 10 ns of the simulations.

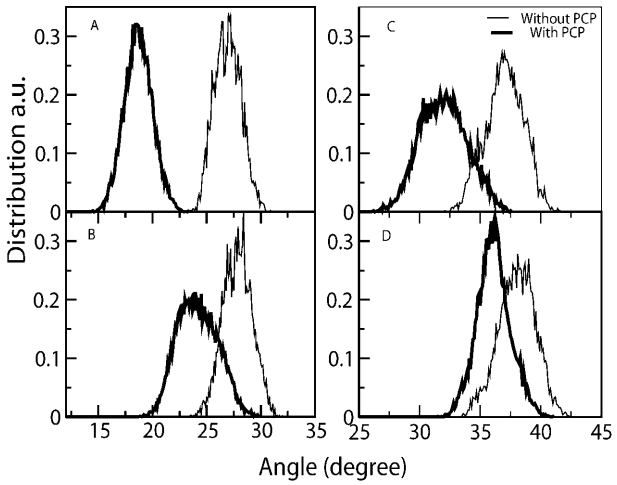

FIGURE 10 Distribution of the tilt angle of the alkyl chains in POPE (*A*, palmitoyl; *B*, oleoyl) and POPC (*C*, palmitoyl; *D*, oleoyl) bilayers in the presence and in the absence of PCP. The distribution of the tilt angle of the alky chains in the lipid bilayers in the presence of PCP was obtained over the last 20 ns and 15 ns of the POPC-A and POPE-A trajectories. The distribution of the tilt angle of the alkyl chains in the pure POPE and POPC bilayers was obtained over the last 10 ns of the pure bilayer simulations.

For both POPC and POPE bilayers, there is a small increase in the order parameter in the presence of PCP. The increase in the S_{CD} order parameter is most pronounced in the region between the carbonyl carbon and the double-bonded carbons of the alkyl chains in both the POPE (Fig. 8, *A–B*) and the POPC (Fig. 8, *C–D*) bilayer. We also calculated the fraction of the dihedral angles in the *trans* conformation along the alkyl chains of the lipid molecules. Fig. 9 shows these fractions for the alkyl chains in the POPC-A (Fig. 9, *A* and *B*) and POPE-A (Fig. 9, *C* and *D*) systems and compares them to the alkyl chains in the pure lipid bilayers. There is no significant difference in the number of *trans* conformations along the alkyl chain dihedrals in the presence of PCP.

Fig. 10 shows the average tilt angle of the palmitoyl and the oleoyl chains in the POPE-A and POPC-A systems and compares them to the average tilt angle of the alkyl chains in the pure lipid bilayers. The average tilt angle of the palmitoyl chains was calculated from the cosine of the angle between the bilayer normal and the average vector, linking the carbon atom at the end of the palmitoyl chain and the carbonyl carbon atom of the same chain. Similarly for the oleoyl chains, the average tilt angle was calculated from the cosine of the angle between the bilayer normal and the average vector linking the double-bonded carbon atom and the carbonyl carbon atom of the same chain.

As shown in Fig. 10, *A–D*, the average tilt angle of the

alkyl chains decreased in the presence of PCP. The average tilt angle of the palmitoyl and oleoyl chains in the POPE bilayer decreased from 27° and 28° in the pure bilayer to 19° and 24°, respectively, in the presence of PCP. For the POPC bilayer, the average tilt angle of the palmitoyl and oleoyl chains decreased from 37° and 38° in the pure bilayer to 32° and 36°, respectively, in the presence of PCP. Thus it seems likely that the increase in the order parameter of the alkyl chains is due to the decrease in the tilt angle of the alkyl chains of the lipid molecules in the presence of PCP.

DISCUSSION

In this article we studied the distribution of PCP, an environmental pollutant, in phospholipid bilayers of POPC and POPE using molecular dynamics computer simulation. The main objectives of the present study were to understand 1), the distribution of PCP in the two types of lipid bilayer; and 2), the effects of PCP on the phospholipid bilayer structure. The present study is a step toward understanding our primary objective, which is the physical basis of membrane modification in microorganisms in the presence of xenobiotic compounds.

There are several lines of evidence that show that PCP prefers to interact with the membrane. The adsorption and partition characteristics of un-ionized PCP as compared to ionized PCP molecules in egg-phosphatidylcholine membrane show that un-ionized PCP has greater affinity to the membranes (Smejtek and Wang, 1993). However, the preferred location of PCP in the bilayer is not known. In a membrane, a solute is not distributed homogeneously, but rather a gradient is formed that varies with the density, polarity, and chain order in the different regions within the membrane (Deyoung and Dill, 1990). Based on the location within the membrane, different molecules have different effects on the membrane structure. For example, simulations have suggested that a difference in the preferred position of halothane (an anesthetic) and hexafluoroethane (a non-immobilizer) in bilayers cause different structural perturbations of the bilayer (Koubi et al., 2001). Thus the structural perturbations of POPC and POPE bilayers caused by PCP should depend on the position of PCP in the bilayers. The present MD simulations of PCP in the POPC and POPE bilayers helped to determine the preferred position of the PCP molecules in the bilayers.

In both the POPC and POPE lipid bilayers, PCP occupies the region between the carbonyl groups and the double-bond groups of the alkyl chains of the lipids, which is a region of high tail density and low free volume compared to the center of the bilayer (Tieleman et al., 1997). The high acyl chain density region imposes spatial restrictions on the motion of the PCP molecules, resulting in the aromatic ring of PCP adopting a preferred orientation aligning with the alkyl chains. The vector normal to the aromatic ring of PCP makes an average angle of 70° and 80° with the bilayer normal in the POPC and POPE bilayer, respectively. The difference in the tilt angle of the aromatic ring of PCP in the two bilayers is due to the difference in the packing density of the lipids in the bilayers and the average tilt angle of the alkyl chains in the bilayers. The area per lipid in the POPE bilayer is less than the POPC bilayer, which implies that lipids pack more tightly in the POPE bilayer compared to the POPC bilayer. Thus there is a greater restriction on the movement of PCP molecules in the POPE bilayer compared to the POPC bilayer, as shown by the broader distribution (Fig. 5 *G*) of the tilt angle of PCP in the POPC lipid bilayer.

Partitioning of nonpolar molecules into bilayers is known to show a ''nonclassical'' hydrophobic effect or ''bilayer effect'' (Seelig and Ganz, 1991). In the bilayer effect, nonpolar solute molecules at room temperature appear to be enthalpy-driven into the lipid bilayer, rather than entropy-driven. The increased ordering of the already constrained alkyl chains by the insertion of a solute molecule results in an entropy loss that opposes solute insertion into the lipid bilayer (Marqusee and Dill, 1986). Thus the hydrophobic entropy opposes solute insertion into water, but the chain entropy opposes solute insertion into the alkyl phase. A favorable enthalpy is thus responsible for the observed partitioning of nonpolar solute into the aligned-chain alkyl phase of the bilayer, which has been attributed to tight packing of solute in that region (DeVido et al., 1998).

Our simulation results are in qualitative agreement with the bilayer effect. The observed partitioning of PCP into the region of high acyl chain density in the lipid bilayer and the parallel alignment of the aromatic ring with the alkyl chains of the lipid molecules in the bilayer are a result of optimal packing of the solute in the dense soft polymer region (Marrink and Berendsen, 1994) of the bilayer, which is what is expected due to the bilayer effect. The hydroxyl group of the PCP molecules found in the hydrocarbon region of the bilayer formed hydrogen bonds with the water and lipid oxygen atoms in the interface region of the bilayer. Thus, through hydrogen bonding, the polar hydroxyl group of PCP can be accommodated in the nonpolar environment of the hydrocarbon region in the lipid bilayers.

Calculation of the deuterium order parameter of the alkyl chains in the presence and absence of PCP showed that in the presence of PCP the lipid chain ordering increased. This increase in the order parameter of the alkyl chains in the presence of PCP is due to the decrease in the tilt angle of the alkyl chains, as the fraction of dihedral angles along the alkyl chains in *trans* conformation does not change significantly in the presence of PCP. The changes in the lipid bilayer structure due to the presence of PCP were similar for POPC and POPE bilayers, with similar distribution of PCP in both the bilayers.

A phosphorus-31 NMR study of the effect of PCP on the physiologies of PCP-degrading *Sphingomonas* species isolates UG25 and UG30 shows that PCP alters the phospholipid composition of the cell membrane (Lohmeier-

Vogel et al., 2001). In these bacterial strains, PCP-pretreated cells had higher cardiolipin (CL) content in the cell membranes than nontreated ones. Bioavailability of an organic compound is important for normal growth of the cell; however, excess of it is known to cause toxic effects to the cell (Sikkema et al., 1995). It has been suggested that higher levels of CL present a physical barrier that controls the amount of compound that can penetrate into the cells (Sikkema et al., 1995), and thus PCP-pretreated bacterial cells with an increased level of CL are subsequently able to tolerate higher PCP concentration. The levels of phosphatidylethanolamine (PE) and phosphatidylcholine (PC) in the PCP-pretreated cells, however, remained the same. In the present MD simulations studies we investigate why the level of PE and PC lipids in cell membranes of PCP-pretreated *Sphingomonas* species remains unchanged. For this purpose we studied the molecular interactions between PCP and POPE, POPC model membranes and rationalized experimental observation based upon these interactions.

Our results show that in both POPE and POPC lipid bilayers, PCP partitions easily into the hydrocarbon core of the bilayer, and thus an increase in the level of PE and PC lipids in the bacterial cell may not provide a favorable physical barrier for penetration of excess PCP molecules that could cause toxicity problems to the cell. Also, PCP seems to effect the phase of the lipid bilayer, converting it from a liquid crystalline phase to more gel like, as suggested by an increase in the order parameter of the alkyl chains, which may also affect the normal functioning of the cell.

CONCLUSIONS

Molecular dynamics computer simulations of the distribution of PCP in POPE and POPC lipid bilayers show that PCP occupies the region between the carbonyl groups and the carbon-carbon double-bond groups of the alkyl chain in the bilayers. PCP increases the rigidity of the lipid bilayers by increasing the deuterium order parameter of the alkyl chains of the lipid molecules and decreasing the average tilt angle of the alkyl chains. The fraction of dihedral angles in *trans* conformation along the lipid chains did not change significantly. The aromatic ring of PCP aligns parallel to the alkyl chains of the lipid molecules in the lipid bilayers, to maximize the interaction with the alkyl chains. The preferred orientation and position of PCP in the lipid bilayers is a result of optimal packing of the solute in the dense ordered chain region of the bilayer. The simulation results are in qualitative agreement with the bilayer effect on the distribution of solute molecules in a lipid bilayer, where the partitioning of a solute between water and the bilayer is enthalpy driven.

The authors thank Dr. H. Lee, Dr. E. Lohmeier-Vogel, and Dr. T. Trevors for their continuing interest in this work. P.M. thanks Dr. Aliste for her assistance with the Gaussian program and Dr. Shepherd for insightful discussions.

This work was supported by the Natural Science and Engineering Research Council of Canada. D.P.T. is a Scholar of the Alberta Heritage Foundation for Medical Research. H.J.V. is an Alberta Heritage Foundation for Medical Research Scientist.

REFERENCES

Aiello, M., O. Moran, M. Pisciotta, and F. Gambale. 1998. Interaction between dihydropyridines and phospholipid bilayers: a molecular dynamics simulation. *Eur. Biophys. J.* 27:211–218.

Anézo, C., A. H. de Vries, H. D. Höltje, D. P. Tieleman, and S. J. Marrink. 2003. Methodological issues in lipid bilayer simulations. *J. Phys. Chem. B.* 107:9424–9433.

Bassolino-Klimas, D., H. E. Alper, and T. R. Stouch. 1995. Mechanism of solute diffusion through lipid bilayer-membranes by molecular-dynamics simulation. *J. Am. Chem. Soc.* 117:4118–4129.

Berendsen, H. J. C., J. P. M. Postma, W. F. van Gunsteren, A. DiNola, and J. R. Haak. 1984. Molecular dynamics with coupling to an external bath. *J. Chem. Phys.* 81:3684–3690.

Berendsen, H. J. C., J. P. M. Postma, W. F. van Gunsteren, and J. Hermans. 1981. Interaction models for water in relation to protein hydration. *In* Intermolecular Forces. B. Pullman, editor. Reidel, Dordrecht, The Netherlands. 331–342.

Berendsen, H. J. C., D. van der Spoel, and R. van Drunen. 1995. GROMACS: a message-passing parallel molecular-dynamics implementation. *Comput. Phys. Commun.* 91:43–56.

Berger, O., O. Edholm, and F. Jähnig. 1997. Molecular dynamics simulations of a fluid bilayer of dipalmitoylphosphatidylcholine at full hydration, constant pressure, and constant temperature. *Biophys. J.* 72: 2002–2013.

Besler, B. H., K. M. Merz, and P. A. Kollman. 1990. Atomic charges derived from semiempirical methods. *J. Comput. Chem.* 11:431–439.

Boden, N., S. A. Jones, and F. Sixl. 1991. On the use of deuterium nuclear-magnetic-resonance as a probe of chain packing in lipid bilayers. *Biochemistry.* 30:2146–2155.

Copley, S. D. 2000. Evolution of a metabolic pathway for degradation of a toxic xenobiotic: the patchwork approach. *Trends Biochem. Sci.* 25:261–265.

Darden, T., D. York, and L. Pedersen. 1993. Particle mesh Ewald: an $N\cdot\log(N)$ method for Ewald sums in large systems. *J. Chem. Phys.* 98:10089–10092.

Denich, T. J., L. A. Beaudette, H. Lee, and J. T. Trevors. 2003. Effect of selected environmental and physico-chemical factors on bacterial cytoplasmic membranes. *J. Microbiol. Methods.* 52:149–182.

DeVido, D. R., J. G. Dorsey, H. S. Chan, and K. A. Dill. 1998. Oil/water partitioning has a different thermodynamic signature when the oil solvent chains are aligned than when they are amorphous. *J. Phys. Chem. B.* 102:7272–7279.

Deyoung, L. R., and K. A. Dill. 1990. Partitioning of nonpolar solutes into bilayers and amorphous *n*- alkanes. *J. Phys. Chem.* 94:801–809.

Diaz, E., A. Ferrandez, M. A. Prieto, and J. L. Garcia. 2001. Biodegradation of aromatic compounds by *Escherichia coli*. *Microbiol. Mol. Biol. Rev.* 65:523–569.

Essmann, U., L. Perera, M. L. Berkowitz, T. Darden, H. Lee, and L. G. Pedersen. 1995. A smooth particle mesh Ewald method. *J. Chem. Phys.* 103:8577–8593.

Feller, S. E. 2000. Molecular dynamics simulations of lipid bilayers. *Curr. Opin. Colloid Interface Sci.* 5:217–223.

Frisch, M. J., G. W. Trucks, H. B. Schlegel, G. E. Scuseria, M. A. Robb, J. R. Cheeseman, V. G. Zakrzewski, J. J. A. Montgomery, R. E. Stratmann, J. C. Burant, S. Dapprich, J. M. Millam, A. D. Daniels, K. N. Kudin, M. C. Strain, O. Farkas, J. Tomasi, V. Barone, M. Cossi, R. Cammi, B. Mennucci, C. Pomelli, C. Adamo, S. Clifford, J. Ochterski, G. A. Petersson, P. Y. Ayala, Q. Cui, K. Morokuma, D. K. Malick, A. D. Rabuck, K. Raghavachari, J. B. Foresman, J. Cioslowski, J. V. Ortiz, B. B. Stefanov,

G. Liu, A. Liashenko, P. Piskorz, I. Komaromi, R. Gomperts, R. L. Martin, D. J. Fox, T. Keith, M. A. Al-Laham, C. Y. Peng, A. Nanayakkara, C. Gonzalez, M. Challacombe, P. M. W. Gill, B. Johnson, W. Chen, M. W. Wong, J. L. Andres, C. Gonzalez, M. Head-Gordon, E. S. Replogle, and J. A. Pople. 1998. Gaussian 98. Gaussian Inc., Pittsburgh, PA.

Grossfield, A., and T. B. Woolf. 2002. Interaction of tryptophan analogs with POPC lipid bilayers investigated by molecular dynamics calculations. *Langmuir*. 18:198–210.

Hazel, J. R., and E. E. Williams. 1990. The role of alterations in membrane lipid composition in enabling physiological adaptation of organisms to their physical environment. *Prog. Lipid Res.* 29:167–227.

Hess, B., H. Bekker, H. J. C. Berendsen, and J. Fraaije. 1997. LINCS: a linear constraint solver for molecular simulations. *J. Comput. Chem.* 18:1463–1472.

Hockney, R. W., S. P. J. Goel, and J. W. Eastwood. 1974. Quite high resolution computer models of a plasma. *J. Comput. Phys.* 14:148–158.

Humphrey, W., A. Dalke, and K. Schulten. 1996. VMD: visual molecular dynamics. *J. Mol. Graph.* 14:33–38.

Jedlovszky, P., and M. Mezei. 2000. Calculation of the free energy profile of H2O, O2, CO, CO2, NO, and CHCl3 in a lipid bilayer with a cavity insertion variant of the Widom method. *J. Am. Chem. Soc.* 122:5125–5131.

Jorgensen, W. L., D. S. Maxwell, and J. Tirado-Rives. 1996. Development and testing of the OPLS all-atom force field on conformational energetics and properties of organic liquids. *J. Am. Chem. Soc.* 118:11225–11236.

König, B., U. Dietrich, and G. Klose. 1997. Hydration and structural properties of mixed lipid/surfactant model membranes. *Langmuir*. 13:525–532.

Koubi, L., M. Tarek, S. Bandyopadhyay, M. L. Klein, and D. Scharf. 2001. Membrane structural perturbations caused by anesthetics and non-immobilizers: a molecular dynamics investigation. *Biophys. J.* 81:3339–3345.

Koubi, L., M. Tarek, M. L. Klein, and D. Scharf. 2000. Distribution of halothane in a dipalmitoylphosphatidylcholine bilayer from molecular dynamics calculations. *Biophys. J.* 78:800–811.

Lindahl, E., B. Hess, and D. van der Spoel. 2001. GROMACS 3.0: a package for molecular simulation and trajectory analysis. *J. Mol. Model.* 7:306–317.

Liu, Y., E. C. Y. Yan, and K. B. Eisenthal. 2001. Effects of bilayer surface charge density on molecular adsorption and transport across liposome bilayers. *Biophys. J.* 80:1004–1012.

Lohmeier-Vogel, E. M., K. T. Leung, H. Lee, J. T. Trevors, and H. J. Vogel. 2001. Phosphorus-31 nuclear magnetic resonance study of the effect of pentachlorophenol (PCP) on the physiologies of PCP-degrading microorganisms. *Appl. Environ. Microbiol.* 67:3549–3556.

Marrink, S. J., and H. J. C. Berendsen. 1994. Simulation of water transport through a lipid membrane. *J. Phys. Chem.* 98:4155–4168.

Marrink, S. J., and H. J. C. Berendsen. 1996. Permeation process of small molecules across lipid membranes studied by molecular dynamics simulations. *J. Phys. Chem.* 100:16729–16738.

Marrink, S. J., R. M. Sok, and H. J. C. Berendsen. 1996. Free volume properties of a simulated lipid membrane. *J. Chem. Phys.* 104: 9090–9099.

Marqusee, J. A., and K. A. Dill. 1986. Solute partitioning into chain molecule interphases: monolayers, bilayer membranes, and micelles. *J. Chem. Phys.* 85:434–444.

Mecozzi, S., A. P. West, and D. A. Dougherty. 1996. Cation-pi interactions in aromatics of biological and medicinal interest: electrostatic potential surfaces as a useful qualitative guide. *Proc. Natl. Acad. Sci. USA.* 93:10566–10571.

Mishra, P., and S. Kaur. 1991. Lipids as modulators of ethanol tolerance in yeast. *Appl. Microbiol. Biotechnol.* 34:697–702.

Mitragotri, S., M. E. Johnson, D. Blankschtein, and R. Langer. 1999. An analysis of the size selectivity of solute partitioning, diffusion, and permeation across lipid bilayers. *Biophys. J.* 77:1268–1283.

Miyamoto, S., and P. A. Kollman. 1992. SETTLE: an analytical version of the SHAKE and RATTLE algorithms for rigid water models. *J. Comput. Chem.* 13:952–962.

Nagle, J. F., and S. Tristram-Nagle. 2000. Structure of lipid bilayers. *Biochim. Biophys. Acta.* 1469:159–195.

Osborne, S. J., J. Leaver, M. K. Turner, and P. Dunnill. 1990. Correlation of biocatalytic activity in an organic-aqueous two-liquid phase system with solvent concentration in the cell membrane. *Enzyme Microb. Technol.* 12:281–291.

Pohorille, A., M. H. New, K. Schweighofer, and M. A. Wilson. 1999. Insights from computer simulations into the interaction of small molecules with lipid bilayers. *Curr. Top. Membr.* 48:49–76.

Pratt, L. R., and A. Pohorille. 2002. Hydrophobic effects and modeling of biophysical aqueous solution interfaces. *Chem. Rev.* 102:2671–2691.

Rand R. P., and V. A. Parsegian. 1989. Hydration forces between phospholipid bilayer. *Biochim. Biophys. Acta.* 988:351–376.

Randa, H. S., L. R. Forrest, G. A. Voth, and M. S. P. Sansom. 1999. Molecular dynamics of synthetic leucine-serine ion channels in a phospholipid membrane. *Biophys. J.* 77:2400–2410.

Saiz, L., S. Bandyopadhyay, and M. L. Klein. 2002. Towards an understanding of complex biological membranes from atomistic molecular dynamics simulations. *Biosci. Rep.* 22:151–173.

Sajbidor, J. 1997. Effect of some environmental factors on the content and composition of microbial membrane lipids. *Crit. Rev. Biotechnol.* 17: 87–103.

Seelig, J., and P. Ganz. 1991. Nonclassical hydrophobic effect in membrane binding equilibria. *Biochemistry.* 30:9354–9359.

Sikkema, J., J. A. M. de Bont, and B. Poolman. 1994. Interactions of cyclic hydrocarbons with biological-membranes. *J. Biol. Chem.* 269:8022–8028.

Sikkema, J., J. A. M. de Bont, and B. Poolman. 1995. Mechanisms of membrane toxicity of hydrocarbons. *Microbiol. Rev.* 59:201–222.

Smejtek, P., and S. R. Wang. 1993. Distribution of hydrophobic ionizable xenobiotics between water and lipid membranes: pentachlorophenol and pentachlorophenate. A comparison with octanol-water partition. *Arch. Environ. Contam. Toxicol.* 25:394–404.

Soderhall, J. A., and A. Laaksonen. 2001. Molecular dynamics simulations of ubiquinone inside a lipid bilayer. *J. Phys. Chem. B.* 105:9308–9315.

Tieleman, D. P., S. J. Marrink, and H. J. C. Berendsen. 1997. A computer perspective of membranes: molecular dynamics studies of lipid bilayer systems. *Biochim. Biophys. Acta Rev. Biomembr.* 1331:235–270.

Trevors, J. T. 1983. Effect of pentachlorophenol on membrane fluidity of *Pseudomonas fluorescens*. *FEMS Microbiol. Lett.* 14:79–94.

van Gunsteren, W. F., S. R. Billeter, A. A. Eising, P. H. Hünenberger, P. Krüger, A. E. Mark, W. R. P. Scott, and I. G. Tironi. 1996. Biomolecular Simulation: The GROMOS96 Manual and User Guide. vdf Hochschulverlag AG an der ETH Zürich, Zürich, Switzerland.

Wang, H., V. Marjomaki, V. Ovod, and M. S. Kulomaa. 2002. Subcellular localization of pentachlorophenol 4-monooxygenase in *Sphingobium chlorophenolicum* ATCC 39723. *Biochem. Biophys. Res. Commun.* 299:703–709.

Xiang, T. X., and B. D. Anderson. 1998. Influence of chain ordering on the selectivity of dipalmitoylphosphatidylcholine bilayer membranes for permeant size and shape. *Biophys. J.* 75:2658–2671.